ORGANIC CHEMISTRY
FRONTIERS

RESEARCH ARTICLE

View Article Online
View Journal | View Issue

Check for updates

Cite this: *Org. Chem. Front.*, 2018, **5**, 2595

One-pot bifunctionalization of unactivated alkenes, P(O)–H compounds, and *N*-methoxypyridinium salts for the construction of β-pyridyl alkylphosphonates†

Yu-Tao He,‡[a] Joonghee Won,‡[a,b] Jiyun Kim,[a,b] Bohyun Park,[a,b] Taehwan Kim,[a,b] Mu-Hyun Baik *[a,b] and Sungwoo Hong *[a,b]

Received 9th July 2018,
Accepted 1st August 2018

DOI: 10.1039/c8qo00689j

rsc.li/frontiers-organic

β-Pyridylphosphines consisting of vicinal pyridine and phosphine groups possess soft acceptor properties of phosphines and hard σ-donor features of pyridines. An efficient method for the synthesis of β-pyridyl alkylphosphonates was developed *via* a three-component reaction between P(O)–H compounds, alkenes and *N*-methoxypyridinium salts under mild conditions. The reaction is thought to occur by the addition of a phosphonyl radical to the alkene to form alkyl radical intermediate, which goes on to add to the *N*- *N*-methoxypyridinium salt. Solvation plays an important role and DFT calculations suggest that the solvation effect is critical in the first step where an alkyl radical intermediate is formed by coupling the phosphonyl radical and the alkene substrate. A plausible mechanism is proposed based on DFT calculations and this novel methodology is applied to a variety of heteroarenium salts and alkene substrates to prepare various synthetically and biologically important β-pyridyl alkylphosphonates.

Introduction

Direct functionalization of pyridine scaffolds has been extensively investigated as an efficient method for the preparation of often complex structures containing pyridine,[1] which are privileged core structures found in numerous natural alkaloids, pharmaceuticals and functional materials.[2] In particular, the β-pyridylphosphine motifs consisting of a vicinal pyridine and a phosphine groups possess the soft π-acceptor properties of a phosphine and the hard σ-donor feature of pyridyl nitrogen at the same time. These molecules are widely employed as versatile ligands for designing transition-metal catalysts.[3] Traditionally, β-pyridylphosphine derivatives may be prepared by Negishi cross-coupling of alkenyl triflate with 2-pyridylzinc, followed by base-promoted addition of the phosphine group into the alkene.[3a,b] Unfortunately, the most straightforward preparation of this useful class of compounds directly by incorporating both phosphine and pyridyl moieties into unsaturated carbon–carbon bonds remained an unmet challenge to date.

Driven by the need for a more efficient synthetic route to β-pyridylphosphine derivatives, we were intrigued by the possibility of developing a three-component cascade reaction[4] using a radical-mediated alkene difunctionalization in a predictable and controllable manner. We speculated that the alkyl radical intermediate **I** generated *in situ* as a result of the addition of a P-centered free radical[5] to the alkene may set the stage for a second radical addition to the pyridine core (Scheme 1). To apply the strategy for the cascade radical phosphonylation and heteroarylation sequence, the radical intermediate **I** should react with the pyridine segment before it can be consumed by H-phosphonate **3** to generate the hydrophosphonylation byproduct **III**. The key difficulty in this approach lies in the poor reactivity of pyridine, and we envisioned that we may overcome this issue if the desired cross-coupling between radical intermediate **I** and pyridine could be engineered to be fast. If successful, such a powerful synthetic strategy would represent a practical and efficient method for the introduction of a phosphine and a pyridyl groups into unactivated alkenes in one operation.

Recently, the Herzon group reported cobalt-mediated alkene functionalizations with *N*-methoxypyridinium salts under hydrogen atom transfer (HAT) conditions that afforded various alkylpyridine products.[6] Due to their relatively strong

[a]*Center for Catalytic Hydrocarbon Functionalizations, Institute for Basic Science (IBS), Daejeon 34141, Korea. E-mail: hongorg@kaist.ac.kr, mbaik2805@kaist.ac.kr*
[b]*Department of Chemistry, Korea Advanced Institute of Science and Technology (KAIST), Daejeon, 34141, Korea*

†Electronic supplementary information (ESI) available: Experimental procedure and characterization of new compounds (^{1}H and ^{13}C NMR spectra). Computational details, optimized Cartesian coordinates of all structures, vibrational frequencies, and energy component. See DOI: 10.1039/c8qo00689j

‡These authors contributed equally to this work.

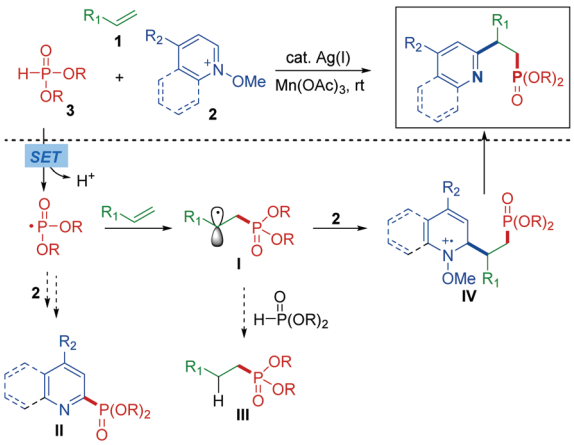

Scheme 1 Design plan: one-pot phosphorylation and heteroarylation of unactivated alkenes.

electrophilic nature, *N*-alkoxyheteroarenium salts can serve as versatile heterocycle surrogates.[7] We speculated that heteroarenium salt **2** may be capable of cross-coupling with intermediate **I**. Interestingly, we discovered in the course of our investigation that the P-centered free radical preferentially reacts with alkene **1** over pyridinium salt **2** to afford alkyl radical **I**, thus preventing the formation of byproduct **II**. This is the first example of an intermolecular, one-pot bifunctionalization of unactivated alkenes, P(O)–H compounds and *N*-methoxypyridinium salts for the construction of β-pyridyl alkylphosphonates under ambient conditions.

Reaction optimization

To test the feasibility of our envisioned approach, we began our studies by investigating the proposed three-component cascade using alkene **1a**, *N*-methoxypyridinium salt **2a** and dimethyl phosphonate (**3a**) as model substrates (see Table S1 in the ESI† for details). The *N*-methoxyheteroarenium salts were easily prepared in high yields by the methylation of the corresponding *N*-oxide.[6,7] We reasoned that silver[8] or copper[9] salts might catalyze the C–P bond construction and promote further radical addition for direct functionalization of the pyridine scaffold. Our initial attempts employing a system consisting of $AgNO_3$ and $Mn(OAc)_3{\cdot}2H_2O$[10] in toluene solution were discouraging because the generated alkyl radical was not active in the desired sequential coupling reaction with *N*-methoxypyridinium salt **2a**. Instead, the byproduct **5a** was obtained presumably *via* hydrophosphonylation along with only a trace amount of the desired product **4a** (Table 1, entry 1). Intriguingly, we found that the solvent has as significant influence on the efficiency of the cascade reactions. For example, the reaction efficacy was considerably improved by using polar solvents such as DMF; the desired three-component product **4a** was obtained in 35% yield (entry 4), indicating that the envisioned cascade process is possible. After extensive screening of various solvents, MeCN was found to be

Table 1 Optimization of the reaction conditions[a]

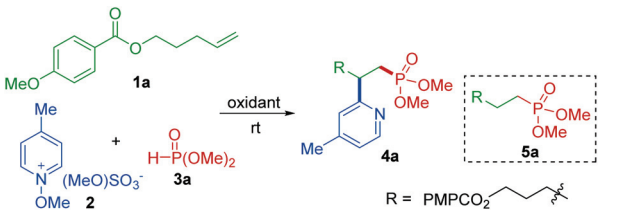

Entry	Oxidant (equiv.)	Solvent	Yield[b] (%) (**4a** : **5a**)
1	$AgNO_3$ (0.2) + $Mn(OAc)_3{\cdot}2H_2O$ (1.5)	Toluene	64 (>5 : 95)
2	$AgNO_3$ (0.2) + $Mn(OAc)_3{\cdot}2H_2O$ (1.5)	Dioxane	71 (16 : 84)
3	$AgNO_3$ (0.2) + $Mn(OAc)_3{\cdot}2H_2O$ (1.5)	DCM	82 (45 : 55)
4	$AgNO_3$ (0.2) + $Mn(OAc)_3{\cdot}2H_2O$ (1.5)	DMF	52 (68 : 32)
5	**$AgNO_3$ (0.2) + $Mn(OAc)_3{\cdot}2H_2O$ (1.5)**	**MeCN**	**88 (81 : 19)**
6	$Mn(OAc)_3{\cdot}2H_2O$ (1.5)	MeCN	31 (71 : 29)
7[c]	$AgNO_3$ (0.2) + $Mn(OAc)_3{\cdot}2H_2O$ (1.5)	MeCN	83 (72 : 28)
8	$Cu(OAc)_2$ (0.2) + $Mn(OAc)_3{\cdot}2H_2O$ (1.5)	MeCN	Trace
9	$AgNO_3$ (0.2) + DTBP (1.5)	MeCN	28 (55 : 45)
10	$AgNO_3$ (0.2) + $K_2S_2O_8$ (1.5)	MeCN	11 (89 : 11)
11	$AgNO_3$ (1.0)	MeCN	22 (78 : 22)
12[d]	$AgNO_3$ (0.2) + $Mn(OAc)_3{\cdot}2H_2O$ (1.5)	MeCN	Trace

[a] Reaction conditions: **1a** (0.2 mmol), **2** (0.5 mmol), **3** (0.4 mmol), oxidant, and solvent (1.0 mL) under nitrogen. [b] Yields were determined by ^{1}H NMR spectroscopy. [c] The reaction was carried out at 60 °C. [d] TEMPO (2.0 equiv.) was added. DTBP = di-*tert*-butyl peroxide.

the most suitable solvent for the cascade transformation, and the desired product **4a** was obtained in 72% at room temperature (entry 5). Subsequent control reactions demonstrated that significantly decreased yields were obtained when the reaction was conducted in the absence of the silver or $Mn(OAc)_3$ (entries 6 and 11). Further studies revealed that increasing the reaction temperature had a negative effect on the selectivity (entry 7). An evaluation of the counterions (BF_4^-, TsO^-, I^- and $MeOSO_3^-$) of the pyridinium salt showed that methyl sulfate was most effective in this process (see Table S1 in the ESI†). Interestingly, negligible reactivity was observed when $AgNO_3$ was replaced with $Cu(OAc)_2$ (entry 8). Various silver salts and oxidants were also screened, and the use of $AgNO_3$ (0.2 equiv.) and $Mn(OAc)_3{\cdot}2H_2O$ (1.5 equiv.) gave the best results. The suppression of the reactivity in the presence of 2,2,6,6-tetramethylpiperidine-1-oxyl (TEMPO) (entry 12) suggests that a radical process may be involved in this transformation. Bases such as K_2CO_3, NaOAc, Cs_2CO_3, and DBU were investigated to facilitate the formation of the P(III),[11] but no beneficial effects were observed.

Computational study

As mentioned above, there are several requirements that must be met for this synthesis strategy to be successful: (i) the terminal alkene must react first with phosphonyl radical (**A1**) (ii) *N*-methoxypyridinium salt should be activated easily to prevent the formation of **5a** as a side product. To better understand these issues and to propose a complete reaction

mechanism, quantum chemical calculations based on density functional theory (DFT) were carried out. All calculations were carried out using the Minnesota functional M06 including Grimme's D3 dispersion correction levels of theory. Optimized structures and vibrational frequencies were obtained using the 6-31G** basis set, and cc-pVTZ(-f) was employed to get precise electronic energies for single point calculations (see the ESI† for computational details). Since the addition of TEMPO shut down the reaction with 90% of the starting material **1a** being recovered (entry 12 in Table 1 and see the ESI† for details), we built a mechanistic model assuming that a transient radical intermediate exists. Specifically, our proposed mechanism begins with the oxidation of **3a** to afford the phosphonyl radical **A1** after deprotonation. The complete reaction energy profile is shown in Fig. 1.

We considered several plausible reactions that the phosphonyl radical **A1** may undergo and found that the lowest energy pathway involves its reaction with the terminal alkene substrate to form **A2**, where a C–P bond is formed. In good agreement with experimental observations, the barrier of this key step associated with the transition state **A1-TS** is only 8.6 kcal mol^{-1}. The alternative reaction with the pyridinium ion traversing **A1′-TS** has a barrier of 11.8 kcal mol^{-1} and would produce **A5**, which will readily undergo deprotonation to restore the aromatic pyridinium moiety assisted by the acetate anion from the $Mn(OAc)_3{\cdot}2H_2O$ additive to yield intermediate **A6**. Therefore, once **A5** is formed, this reaction pathway becomes practically irreversible and it will be not possible to regenerate **A1**.

Thus, these DFT results suggest that the initial C–P bond forming step that shows a 3.2 kcal mol^{-1} preference for engaging the alkene over pyridinium is responsible for the selectivity. Although the barriers computed using DFT methods must be evaluated with some caution and are not to be taken as quantitatively reliable, the decisive difference in transition state energy is meaningful and is in good qualitative agreement with the experimentally observed high selectivity.

To better understand the chemical reason for the computed selectivity, we carried out an energy decomposition and fragment energy calculations. Fig. 2 compares the different components of the solution phase free energy. Interestingly, the electronic energy (ΔE) of **A1′-TS** is ~3.0 kcal mol^{-1} lower than

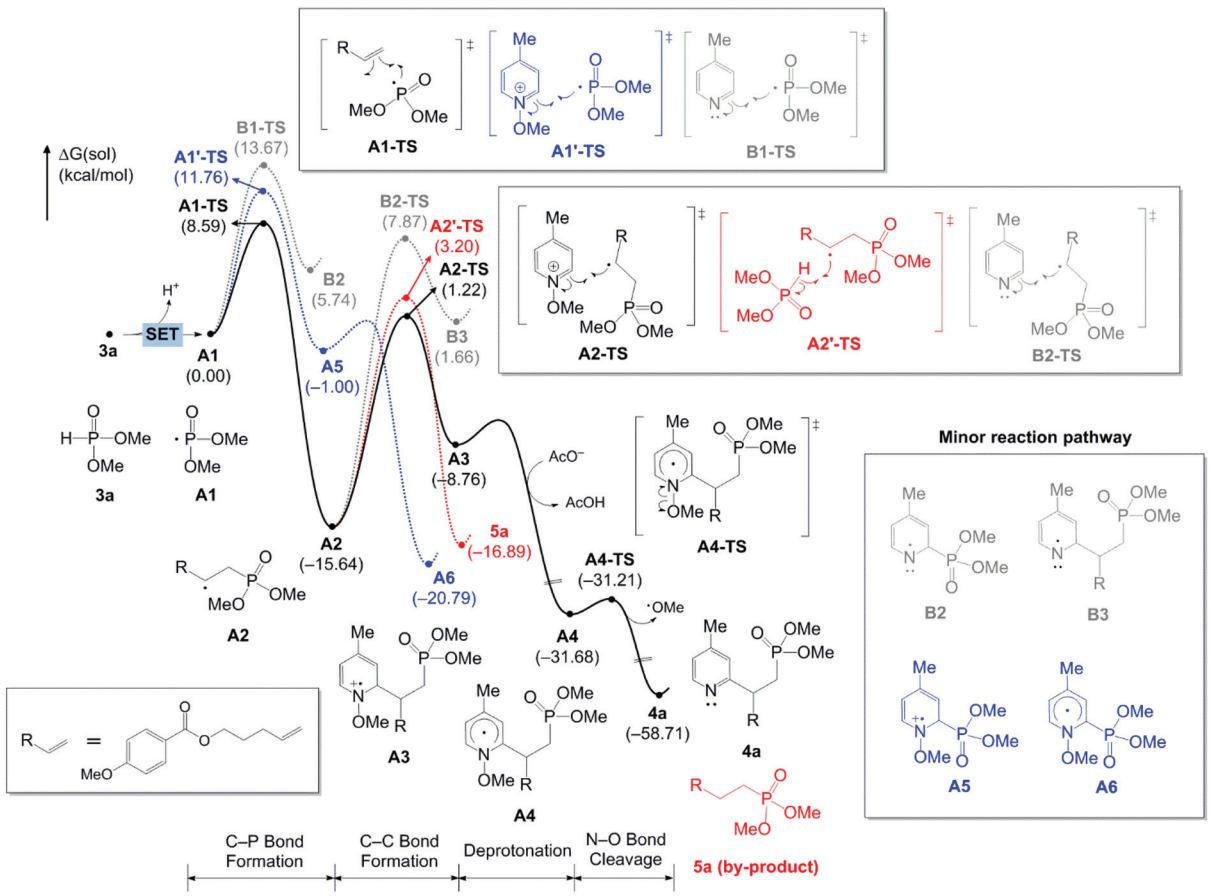

Fig. 1 Free energy profile for the formation of β-pyridyl alkylphosphonate that is described with black solid line. Blue and red traces represent the C–P bond formation of pyridinium and side-product generating step respectively. Grey trace is for pyridine case instead of pyridinium.

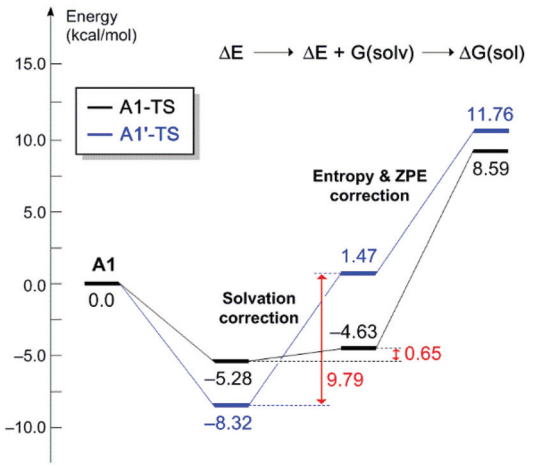

Fig. 2 Energy difference between **A1-TS** and **A1′-TS** at electronic energy (Δ*E*), solvation corrected electronic energy (Δ*E* + *G*(solv)), and entropy corrected Gibbs free energy (Δ*G*(sol)).

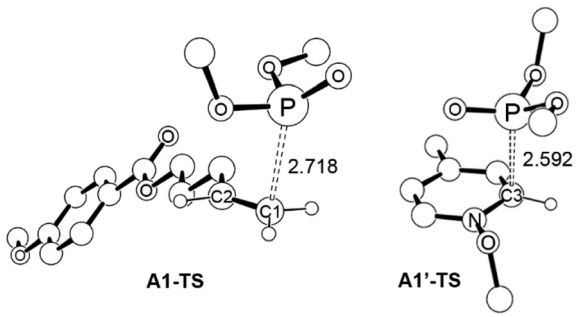

Fig. 3 Optimized structures of **A1-TS** and **A1′-TS**. Non-essential atoms have been omitted for clarity.

that of **A1-TS**, but the energy ordering is reversed due to higher penalty of the solvation energy (*G*(solv)) in **A1′-TS**. The solvation energies of terminal alkene and phosphonyl radical (**A1**) are −9.9 and −9.1 kcal mol^{-1}, respectively, to combine to −18.9 kcal mol^{-1}. The solvation energy of **A1-TS** is −18.3 kcal mol^{-1} giving a solvation penalty of only 0.7 kcal mol^{-1} for the **A1** → **A1-TS** step. The cationic pyridinium ion shows a greater solvation energy of −52.6 kcal mol^{-1}, affording a total solvation energy of −61.6 kcal mol^{-1} for the reactants of the alternative reaction. Interestingly, the solvation energy of **A1′-TS** is only −51.8 kcal mol^{-1}, resulting in a solvation energy penalty of 9.8 kcal mol^{-1}, which inverts the electronic energy ordering to finally give a preference of 6.1 kcal mol^{-1} for **A1-TS**. Entropy correction only plays a minor role and adjusts the final free energy difference to 3.2 kcal mol^{-1}.

Because the energy difference of the two transition states is of central importance, we analyzed the electronic and solvation corrected energy differences in greater detail, as shown in the ESI† (see Fig. S1 in the ESI† for details). In essence, we found that the terminal alkene and **A1** substrates can react with each other with minimal structural change estimated to be 1.4 kcal mol^{-1}, but the intermolecular interaction is also weak at −6.7 kcal mol^{-1} for **A1-TS**. These energies are easy to understand considering that the C–P bond is formed by a radical attack on a fairly localized π-orbital, which should cause only minimal structural change. A much more pronounced electronic change is needed to engage pyridinium, as the initially delocalized and aromatic π-orbital must be forced to localize and match the localized phosphonyl radical **A1**. As a consequence, the structural distortion in **A1′-TS** is more severe and demands 4.2 kcal mol^{-1} with interaction energy being also greater at −12.5 kcal mol^{-1}, to ultimately afford a lower electronic energy for **A1′-TS** over **A1-TS**. As shown in Fig. 3, the optimized P–C distances in **A1-TS** and **A1′-TS** are 2.72 and 2.59 Å, respectively, in good agreement with the much stronger interaction energy in **A1′-TS** over that of **A1-TS**. These computed results are internally consistent and easy to understand, given the localized *vs.* delocalized nature of the π-orbitals in the alkene and pyridinium substrates, respectively.

On first sight, the dramatic difference of the solvation effect on the two transition state energies is puzzling, but a closer inspection reveals a very simple reason for why the transition state **A1′-TS** with a solvation energy of −51.8 kcal mol^{-1} is nearly 10 kcal mol^{-1} disfavored compared to the reactant states **A1** and the pyridinium substrate with solvation energies of −9.1 and −52.6 kcal mol^{-1}, respectively (see Table S3 in the ESI†). The solvation energy of the pyridinium ion is mainly determined by the positive charge and as the new P–C bond is formed, that positive charge is distributed across the whole molecule, leading to a solvation energy that is essentially identical to that of the pyridinium substrate. Similarly, the P–C coupled intermediate **A5** also has a similar solvation energy of −53.3 kcal mol^{-1}. Thus, in this case, the pyridinium ion acts as an electrophile and the radical **A1** acts as a nucleophile.

Electron-deficient *N*-heteroarenium substrates have been widely employed to attain different types of heteroarylation reactions. The most popular example is the Minisci reaction, which gives access to protonated heteroarenes in acidic conditions to furnish C–C bonds between the heteroarene and a radical generated by various reagents (Minisci,[12] borono-Minisci,[13] using zinc sulphinate salts,[14] *etc.*). Of particular interest in these reactions is that the electron-deficient *N*-heteroarenium is utilized as an electrophile, whereas the carbonyl radical behaves like a nucleophile, similar to what we mentioned above. There are only a few fundamental investigations of reactions between radicals and closed-shell molecules. Fundamentally, radicals can act both as electrophiles and nucleophiles, but specific examples that demonstrate these ambivalent reactivity characteristics are rare.[15] The theoretical analysis of the P–C coupling reactions described above are interesting, as they suggest that the phosphonyl radical acts as a nucleophile when reacting with the pyridinium cation, whereas it is clearly an electrophile when reacting with the alkenyl substrate.

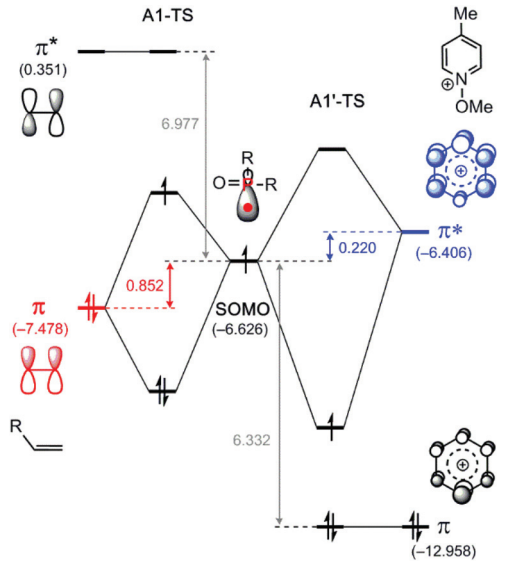

Fig. 4 Qualitative MO diagram of radical interaction with terminal alkene or pyridinium. Alkene **1a** is used for terminal alkene substrate and energies are given in eV (see Fig. S2–S4 in the ESI† for details).

Whether the phosphonyl radical acts as a nucleophile or an electrophile is determined by the shapes and energies of the frontier orbitals of the reactants, where the singly occupied molecular orbital (SOMO) of the phosphonyl radical plays a central role, as is illustrated in Fig. 4. Unsurprisingly, this SOMO is mostly a P-centered sp-hybrid orbital at −6.63 eV. The highest occupied π and lowest unoccupied π* MOs of the alkene substrate are found −7.48 and +0.35 eV, respectively, whereas the analogous orbitals of the pyridinium substrate are found at −12.96 and −6.41 eV, respectively. Given these orbital energies, it is easy to understand that the phosphonyl SOMO preferentially attacks the occupied π orbital of the alkenyl substrate, shown in red in Fig. 4, whereas the unoccupied π* MO of the pyridinium cation is energetically the only plausible target, highlighted in blue. As a consequence, the radical attack on the olefin is a 2-orbital-3-electron interaction, where the single electron is placed in a P–C antibonding orbital, but the reaction with pyridinium is a 2-orbital-1-electron interaction and the single electron is placed in a P–C bonding orbital. This finding is in good agreement with the energies and bond lengths discussed above and give for the first time an in-depth comparison of the MO-interactions when a radical acts as an electrophile and a nucleophile.

In summary, our DFT-calculations predict that **A1** will preferentially react with the alkene substrate to selectively afford the intermediate **A2** under the experimentally probed conditions, as illustrated in Fig. 1. To push the reaction forward and form the bifunctionalized product, pyridinium is engaged traversing the transition state **A2-TS** at 1.2 kcal mol^{-1} to generate the intermediate **A3** at −8.8 kcal mol^{-1} with a step barrier of 16.9 kcal mol^{-1}. Experimentally, the hydrogen quenched byproduct **5a** was observed, and we propose that this undesired product is the result of a hydrogen atom transfer from an equivalent of the dimethyl phosphonate (**3a**) to intermediate **A2**. We were able to find a transition state, **A2′-TS**, for this process at 3.2 kcal mol^{-1}, resulting in a predicted barrier that is 2 kcal mol^{-1} higher than the reaction with pyridinium, as highlighted in red in Fig. 1. The main reaction energy pathway continues from **A3** *via* acetate mediated deprotonation to form the neutral pyridinyl radical species **A4**, which is of course unstable and readily undergoes nearly barrierless homolytic cleavage of N–O bond to form the desired product **4a** at −58.7 kcal mol^{-1} and liberate a methoxy radical.[16] The resulting methoxy radical is released as methanol,[6] or further oxidized to formaldehyde by the action of $Mn(OAc)_3{\cdot}2H_2O$.

Substrate scope

With the detailed mechanistic proposal for the one-pot synthesis of β-pyridyl alkylphosphonate **4a** in hand, we explored the substrate scope of *N*-methoxypyridinium salts to test the generality of this reaction. Compared to more classical reactions that do not involve radicals, these reactions should show much greater functional group tolerance, as the radical reactions are less strongly impacted by inductive effects of functional group. Our proposed mechanism suggests that the initial P–C bond formation is relatively easy, but the second step involving the C–C coupling between the original alkenyl-carbon and the pyridinium moiety is more challenging. Thus, if there is a strong difference in reactivity, we expect it to be at the second step traversing the C–C coupling transition state **A2-TS**. Consequently, we chose to start our investigation by functionalizing the pyrimidinium moiety first. The results are summarized in Table 2. We were delighted to observe that the phosphono-heteroarylation of 4-methoxyphenyl hex-5-enoate (**1a**) works well for a range of substituted *N*-methoxypyridinium salts and readily afforded the desired β-pyridyl alkylphosphonates. In general, *N*-methoxypyridinium derivatives bearing C-4 substituents (methyl, phenyl, chloro, methyl ketone, trifluoromethyl, ester, and cyano) underwent C-2 alkylation exclusively and gave single products (**4a–4g**). Reactions of pyridinium substrates bearing ester groups at the C-2 or C-3 positions proceeded smoothly, but a mixture of regioisomers was produced (**4h** and **4i**). Interestingly, when a substrate containing a C-3 methoxy group was employed, the C-6 alkylation product **4k** was exclusively obtained in 52% yield. The *N*-methoxy pyridazinium salt also worked well to provide pyridazine derivative **4n** in 78% yield with 2.7 : 1 C-3/C-4 selectivity. Further exploration demonstrated that quinoline derivatives were suitable substrates and afford the desired products in moderate to good yields (**4o–4r**). Next, the scope with regard to phosphonates was investigated, and a range of phosphonates (**4s–4v**) and dialkyl phosphine (**4w**) were determined to be suitable coupling partners for this transformation. *N*-Methoxyimidazolium salt could be employed as the

Table 2 Substrate scope of *N*-methoxyheteroarenium salts[a,b]

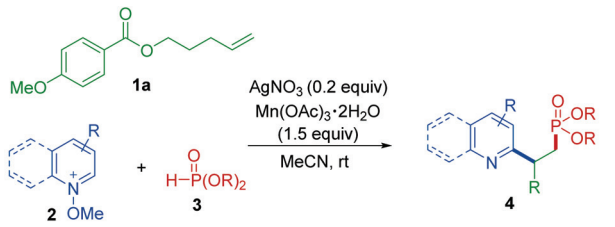

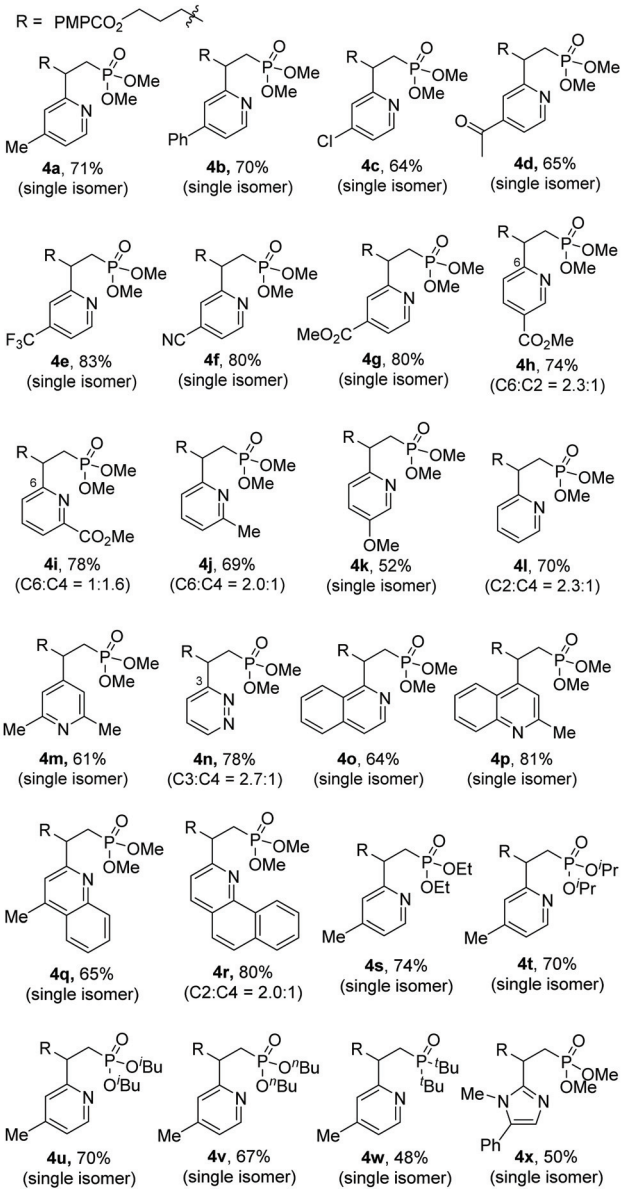

[a] Reaction conditions: **1a** (0.2 mmol), **2a** (0.5 mmol), **3a** (0.4 mmol), $AgNO_3$ (0.2 equiv.), and $Mn(OAc)_3{\cdot}2H_2O$ (1.5 equiv.) in MeCN (1.0 mL) at rt for 30 h under N_2. [b] Yields of the isolated products; the ratios of the isomers were determined by ^1H NMR spectroscopy of the crude product mixtures.

Table 3 Substrate scope for alkenes[a,b]

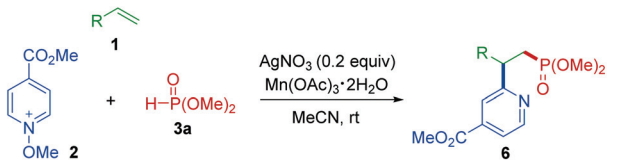

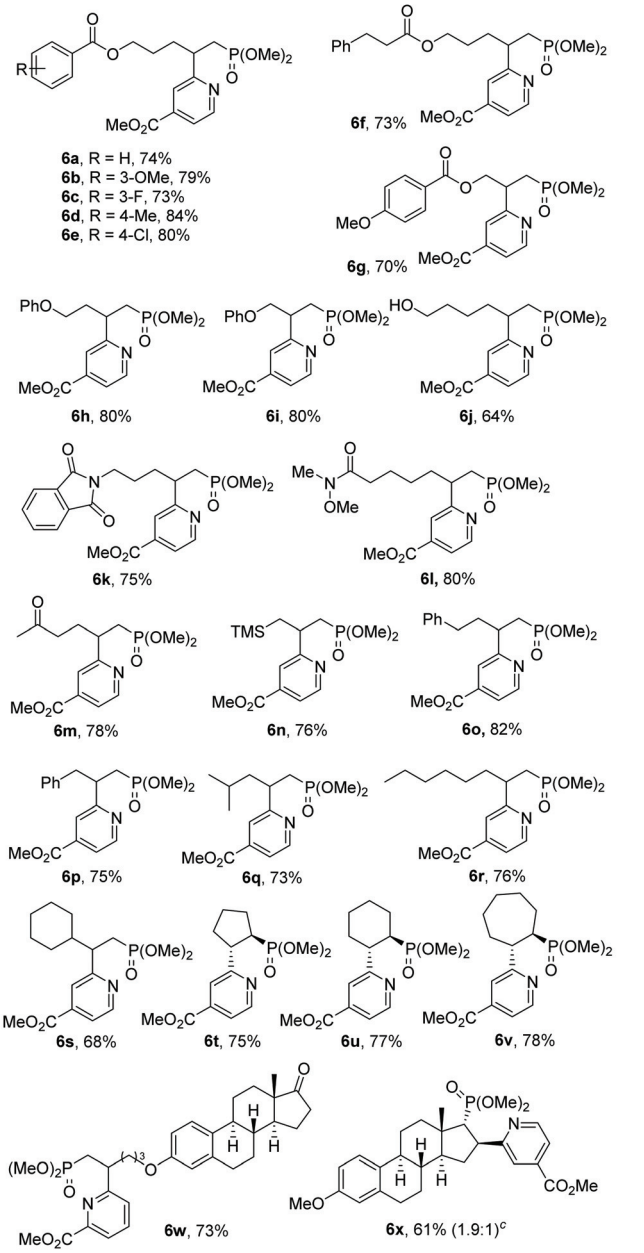

[a] Reaction conditions: **1a** (0.2 mmol), **2a** (0.5 mmol), **3a** (0.4 mmol), $AgNO_3$ (0.2 equiv.), and $Mn(OAc)_3{\cdot}2H_2O$ (1.5 equiv.) in MeCN (1.0 mL) at rt for 30 h under N_2. [b] Yields of the isolated products. [c] Regioisomeric ratio. The structural assignment was based on the analysis of 2D-NMR (COSY, NOE, HSQC, and HMBC). See the ESI for details.

heteroarene source, which afforded the corresponding coupling product **4x**.

Next, we turned our attention to different alkene derivative with the expectation that the scope should be broad, as the initial P–C step is computed to be easy and we do not expect standard functionalizations to change the shape or the energy of the alkenyl π-orbital enough to diminish its interaction with the P-centered radical orbital. The results are summarized in Table 3 and confirm this expectation. The use of alkene substrates bearing a wide range of functional groups, including ester, phthalimide, Weinreb amide, ether, trimethylsilane, and ketone moieties, was well tolerated in this reaction, and the corresponding β-pyridyl alkylphosphonates were produced in satisfying yields. Importantly, the alkene with a hydroxyl group was also well tolerated in the reaction (**6j**), and the cyclized ether ring product was not observed, which indicated that a carbocation intermediate is either not formed at all or the possible cyclization reaction is too slow to compete with the main reaction trajectory. The current protocol could also be extended to the functionalization of cyclic internal alkenes to afford the corresponding products (**6t–6v**), which can be used in the field of catalysis as P,N-ligands.[3] Finally, we assessed the potential of this convenient one-pot method for preparing more complex substrates, such as estrone derivatives. Gratifyingly, we found that such useful extension is possible, yielding desired products **6w** and **6x** in 73% and 61% (1.9 : 1), respectively.

involved in this transformation, which we propose to be the **A2** intermediate.

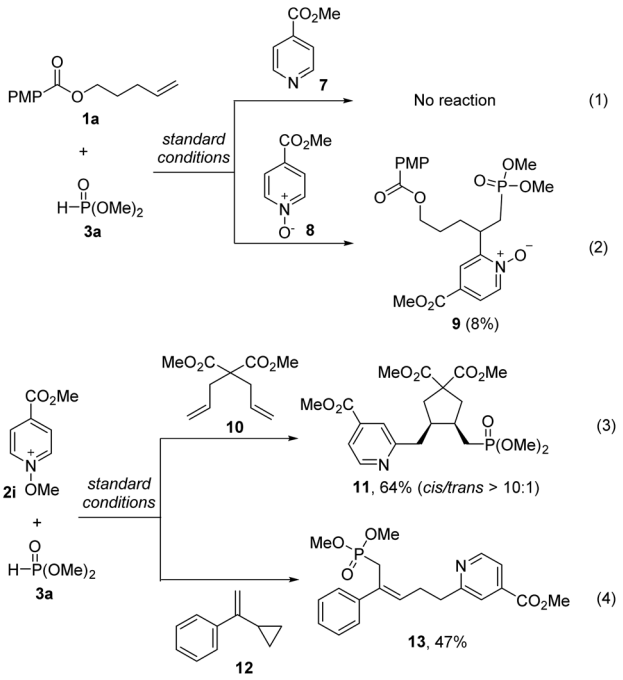

Control experiments

Several control experiments were performed to further test the proposed reaction mechanism. Our conceptual analysis of the C–C coupling highlights that cationic charge and the electrophilicity of pyridinium is key to this reaction. The frontier orbitals of the neutral pyridine analogue are notably shifted and should out of range for the P–C coupled intermediate to engage (see Fig. S4 in the ESI† for details). Thus, we subjected the analogous substrates pyridine **7** and pyridine *N*-oxide **8** to standard reaction conditions. As anticipated, pyridine gave no reaction (eqn (1)), whereas the pyridine *N*-oxide **8** can of course be converted into the corresponding product **9**, albeit in only 8% yield (eqn (2)). This observation is also easy to understand using our proposed mechanism: as shown in Fig. 2, we suggest that the electrophilicity of the pyridinium substrate is critical. Whereas the pyridine *N*-oxide **8** offers similar electronic structure patterns, its electrophilicity is notably reduced when compared to that of a pyridinium species. Next, two more reactions were carried out to provide evidence for the radical-based process. The reaction of diene **10** underwent a cascade reaction under the optimized conditions and gave the cyclized product **11** (64% yield) in predominantly *cis*-configuration (eqn (3)). In addition, the ring-opened product **13** was generated from the reaction with vinylcyclopropane **12** (eqn (4)). These observations support the notion that a C-centered radical is

Conclusions

In conclusion, we developed a highly efficient phosphonoheteroarylation reaction of unactivated alkenes through a one-pot bifunctionalization process to give access to synthetically and biologically important β-pyridylphosphine structural motifs. We found that the solvent plays a fundamentally important and non-trivial role. MeCN was found to be the most suitable solvent. Combining experimental and computational methods, we derived a complete and detailed mechanistic understanding of the origin of the selective reaction pathway to ultimately generate desired product. In addition, an intriguing novel concept for how the phosphonyl radical engages the alkene in an electrophilic and the pyridinium cation in a nucleophilc fashion was suggested. The synthetic potential of this method was demonstrated by the expeditious synthesis of new P,N-ligands and the late-stage modification of estrone derivatives. The method is compatible with a broad range of alkene substrates and *N*-heteroarenium salts (pyridinium, quinolinium, isoquinolinium, and pyridazinium salts), providing a facile synthetic route to synthetically and biologically important β-pyridyl alkylphosphonates with good functional group tolerance. Finally, this study demonstrates the synergistic effect of combining computational and experimental work in a fully integrated mechanistic study to develop a practically useful synthetic methodology with a precise understanding of the mechanism.

Conflicts of interest

There are no conflicts to declare.

Acknowledgements

This research was supported financially by Institute for Basic Science (IBS-R010-G1 and IBS-R010-D1).

Notes and references

1 For selected examples of pyridine functionalizations, see: (*a*) J. C. Lewis, R. G. Bergman and J. A. Ellman, *J. Am. Chem. Soc.*, 2007, **129**, 5332; (*b*) C.-C. Tsai, W.-C. Shih, C.-H. Fang, C.-Y. Li, T.-G. Ong and G. P. A. Yap, *J. Am. Chem. Soc.*, 2010, **132**, 11887; (*c*) F. O'Hara, D. G. Blackmond and P. S. Baran, *J. Am. Chem. Soc.*, 2013, **135**, 12122; (*d*) J. Gui, Q. Zhou, C. M. Pan, Y. Yabe, A. C. Burns, M. R. Collins, M. A. Ornelas, Y. Ishihara and P. S. Baran, *J. Am. Chem. Soc.*, 2014, **136**, 4853; (*e*) J. Jin and D. W. C. Macmillan, *Angew. Chem., Int. Ed.*, 2015, **54**, 1565; (*f*) J. Jin and D. W. C. Macmillan, *Nature*, 2015, **525**, 87; (*g*) G. L. Gao, W. Xia, P. Jain and J. Q. Yu, *Org. Lett.*, 2016, **18**, 744; (*h*) M. C. Hilton, R. D. Dolewski and A. McNally, *J. Am. Chem. Soc.*, 2016, **138**, 13806; (*i*) J. P. Lutz, S. T. Chau and A. G. Doyle, *Chem. Sci.*, 2016, **7**, 4105; (*j*) S. Yamada, K. Murakami and K. Itami, *Org. Lett.*, 2016, **18**, 2415; (*k*) W. Jo, J. Kim, S. Choi and S. H. Cho, *Angew. Chem., Int. Ed.*, 2016, **55**, 9690; (*l*) P. S. Fier, *J. Am. Chem. Soc.*, 2017, **139**, 9499; (*m*) R.-B. Hu, S. Sun and Y. Su, *Angew. Chem., Int. Ed.*, 2017, **56**, 10877.

2 (*a*) Y. Yamaguchi, S. Kobayashi, S. Miyamura, Y. Okamoto, T. Wakamiya, Y. Matsubara and Z. Yoshida, *Angew. Chem., Int. Ed.*, 2004, **43**, 366; (*b*) P. Jakubec, A. Hawkins, W. Felzmann and D. J. Dixon, *J. Am. Chem. Soc.*, 2012, **134**, 17482; (*c*) C. K. Prier, D. A. Rankic and D. W. C. MacMillan, *Chem. Rev.*, 2013, **113**, 5322; (*d*) A. A. Altaf, A. Shahzad, Z. Gul, N. Rasool, A. Badshah, B. Lal and E. Khan, *J. Drug Des. Med. Chem.*, 2015, **1**, 1.

3 (*a*) T. Bunlaksananusorn, K. Polborn and P. Knochel, *Angew. Chem., Int. Ed.*, 2003, **42**, 3941; (*b*) T. Bunlaksananusorn and P. Knochel, *J. Org. Chem.*, 2004, **69**, 4595; (*c*) F. Y. Kwong and K. S. Chan, *Organometallics*, 2001, **20**, 2570; (*d*) F. Y. Kwong, Q. Yang, T. C. W. Mak, A. S. C. Chan and K. S. Chan, *J. Org. Chem.*, 2002, **67**, 2769; (*e*) S. Chen, J. K.-P. Ng, S. A. Pullarkat, F. Liu, Y. Li and P.-H. Leung, *Organometallics*, 2010, **29**, 3374; (*f*) O. Loiseleur, M. Hayashi, M. Keenan, N. Schmees and A. Pfaltz, *J. Organomet. Chem.*, 1999, **576**, 16; (*g*) M. P. Carroll and P. J. Guiry, *Chem. Soc. Rev.*, 2014, **43**, 819.

4 For selected examples, see: (*a*) N. Chatani, S. Fujii, Y. Yamasaki, S. Murai and N. Sonoda, *J. Am. Chem. Soc.*, 1986, **108**, 7361; (*b*) D. Leca, L. Fensterbank, E. Lacôte and M. Malacria, *Chem. Soc. Rev.*, 2005, **34**, 859; (*c*) M. Jeganmohan, S. Bhuvaneswari and C.-H. Cheng, *Angew. Chem., Int. Ed.*, 2009, **48**, 391; (*d*) L. Zhou, C. K. Tan, J. Zhou and Y.-Y. Yeung, *J. Am. Chem. Soc.*, 2010, **132**, 10245; (*e*) W. Wei and J. X. Ji, *Angew. Chem., Int. Ed.*, 2011, **50**, 9097; (*f*) W. Zhao, Z. Wang and J. Sun, *Angew. Chem., Int. Ed.*, 2012, **51**, 6209; (*g*) J. Zhou, L. Zhou and Y.-Y. Yeung, *Org. Lett.*, 2012, **14**, 5250; (*h*) Z. Chen, B. Wang, Z. Wang, G. Zhu and J. Sun, *Angew. Chem., Int. Ed.*, 2013, **52**, 2027; (*i*) B. H. Rotstein, S. Zaretsky, V. Rai and A. K. Yudin, *Chem. Rev.*, 2014, **114**, 8323; (*j*) L. K. B. Garve and D. B. Werz, *Org. Lett.*, 2015, **17**, 596; (*k*) X.-Q. Pan, J.-P. Zou, W.-B. Yi and W. Zhang, *Tetrahedron*, 2015, **71**, 7481; (*l*) T. Shen, Y. Zhang, Y.-F. Liang and N. Jiao, *J. Am. Chem. Soc.*, 2016, **138**, 13147.

5 The review on P-centered radical difunctionalizations: Y. Gao, G. Tang and Y. Zhao, *Phosphorus, Sulfur Silicon Relat. Elem.*, 2017, **192**, 589.

6 (*a*) X. Ma and S. B. Herzon, *J. Am. Chem. Soc.*, 2016, **138**, 8718; (*b*) X. Ma, H. Dang, J. A. Rose, P. Rablen and S. B. Herzon, *J. Am. Chem. Soc.*, 2017, **139**, 5998.

7 (*a*) R. B. Katz, J. Mistry and M. B. Mitchell, *Synth. Commun.*, 1989, **19**, 317; (*b*) M. A. A. Biyouki, R. A. J. Smith, J. J. Bedford and J. P. Leader, *Synth. Commun.*, 1998, **28**, 3817; (*c*) V. Quint, F. Morlet-Savary, J. F. Lohier, J. Lalevee, A. C. Gaumont and S. Lakhdar, *J. Am. Chem. Soc.*, 2016, **138**, 7436.

8 For selected recent examples of Ag-catalyzed generation of P-centered radicals, see: (*a*) C. Zhang, Z. Li, L. Zhu, L. Yu, Z. Wang and C. Li, *J. Am. Chem. Soc.*, 2013, **135**, 14082; (*b*) Y.-M. Li, M. Sun, H.-L. Wang, Q.-P. Tian and S.-D. Yang, *Angew. Chem., Int. Ed.*, 2013, **52**, 3972; (*c*) Z.-Z. Zhou, D.-P. Jin, L.-H. Li, Y.-T. He, P.-X. Zhou, X.-B. Yan, X.-Y. Liu and Y.-M. Liang, *Org. Lett.*, 2014, **16**, 5616; (*d*) B. Zhang, C. G. Daniliuc and A. Studer, *Org. Lett.*, 2014, **16**, 250; (*e*) H. Zhang, Z. Gu, Z. Li, C. Pan, W. Li, H. Hu and C. Zhu, *J. Org. Chem.*, 2016, **81**, 2122; (*f*) H.-L. Hua, B.-S. Zhang, Y.-T. He, Y.-F. Qiu, X.-X. Wu, P.-F. Xu and Y.-M. Liang, *Org. Lett.*, 2016, **18**, 216; (*g*) J. A. Li, P. Z. Zhang, K. Liu, A. Shoberu, J. P. Zou and W. Zhang, *Org. Lett.*, 2017, **19**, 4704.

9 For selected recent examples of Cu-catalyzed generation of P-centered radicals, see: (*a*) J. Ke, Y. Tang, H. Yi, Y. Li, Y. Cheng, C. Liu and A. Lei, *Angew. Chem., Int. Ed.*, 2015, **54**, 6604; (*b*) Y. Gao, X. Li, W. Chen, G. Tang and Y. Zhao, *J. Org. Chem.*, 2015, **80**, 11398; (*c*) H.-Y. Zhang, L.-L. Mao, B. Yang and S.-D. Yang, *Chem. Commun.*, 2015, **51**, 4101; (*d*) H. Zhang, W. Li and C. Zhu, *J. Org. Chem.*, 2017, **82**, 2199; (*e*) X.-S. Li, Y.-P. Han, X.-Y. Zhu, M. Li, W.-X. Wei and Y.-M. Liang, *J. Org. Chem.*, 2017, **82**, 11636.

10 For selected examples of Mn-mediated generation of P-centered radicals, see: (*a*) T. Kagayama, A. Nakano, S. Sakaguchi and Y. Ishii, *Org. Lett.*, 2006, **8**, 407; (*b*) X.-Q. Pan, J.-P. Zou, G.-L. Zhang and W. Zhang, *Chem. Commun.*, 2010, **46**, 1721; (*c*) X.-Q. Pan, L. Wang, J.-P. Zou and W. Zhang, *Chem. Commun.*, 2011, **47**, 7875;

(*d*) F. Zhang, L. Wang, C. Zhang and Y. Zhao, *Chem. Commun.*, 2014, **50**, 2046; (*e*) S.-F. Zhou, D.-P. Li, K. Liu, J.-P. Zou and O. T. Asekun, *J. Org. Chem.*, 2015, **80**, 1214; (*f*) P.-Z. Zhang, L. Zhang, J.-A. Li, A. Shoberu, J.-P. Zou and W. Zhang, *Org. Lett.*, 2017, **19**, 5537.

11 (*a*) B. Janesko, H. C. Fisher, M. J. Bridle and J.-L. Montchamp, *J. Org. Chem.*, 2015, **80**, 10025; (*b*) Y. Liu, X. Fan, Z. H. Li and H. Wang, *Chem. Commun.*, 2017, **53**, 10890.

12 For Minisci reaction, see: (*a*) F. Minisci, *Synthesis*, 1973, 1; (*b*) F. Minisci, E. Vismara and F. Fontana, *Heterocycles*, 1989, **28**, 489; (*c*) F. Minisci, F. Fontana and E. Vismara, *J. Heterocycl. Chem.*, 1990, **27**, 79; (*d*) M. A. J. Duncton, *MedChemComm*, 2011, **2**, 1135.

13 For borono-Minisci reaction, see: (*a*) I. B. Seiple, S. Su, R. A. Rodriguez, R. Gianatassio, Y. Fujiwara, A. L. Sobel and P. S. Baran, *J. Am. Chem. Soc.*, 2010, **132**, 13194; (*b*) Y. Fujiwara, V. Domingo, I. B. Seiple, R. Gianatassio, D. M. Bel and P. S. Baran, *J. Am. Chem. Soc.*, 2011, **133**, 3292; (*c*) N. R. Patel and R. A. Flowers, *J. Am. Chem. Soc.*, 2013, **135**, 4672.

14 Y. Fujiwara, J. A. Dixon, F. O'Hara, E. D. Funder, D. D. Dixon, R. A. Rodriguez, R. D. Baxter, B. Herle, N. Sach, M. R. Collins, Y. Ishihara and P. S. Baran, *Nature*, 2012, **492**, 95.

15 (*a*) F. D. Vleeschouwer, V. V. Speybroeck, M. Waroquier, P. Geerlings and F. D. Proft, *Org. Lett.*, 2007, **9**, 2721; (*b*) L. R. Domingo and P. Pérez, *Org. Biomol. Chem.*, 2013, **11**, 4350; (*c*) E. H. Krenske and C. H. Schiesser, *Org. Biomol. Chem.*, 2008, **6**, 854; (*d*) R. I. J. Amos, J. A. Smith, B. F. Yates and C. H. Schiesser, *Tetrahedron*, 2010, **66**, 7600.

16 I. Kim, M. Min, D. Kang, K. Kim and S. Hong, *Org. Lett.*, 2017, **19**, 1394.